IEEE Sensors Council

An Efficient Calibration Method of Line Structured Light Vision Sensor in Robotic Eye-in-Hand System

Zhe Wang, Junfeng Fan, Fengshui Jing, Sai Deng, Mingyang Zheng, and Min Tan

***Abstract*—For line structured light vision sensor in robotic eye-in-hand system, the calibration of camera parameters, robot hand eye parameters and structured light plane parameters is an indispensable procedure before conducting 3-D measurement. Traditionally, these three sets of parameters are calibrated separately, making the calibration process complicated and inefficient. To address this, an efficient calibration method is proposed in this paper. By changing the poses of robot and calibration target, a set of images of the calibration target is captured, upon which the camera calibration is conducted. The extrinsic parameters obtained from camera calibration are utilized in the calibration of the structured light plane parameters and hand eye parameters, using the same set of images. Therefore, the three sets of parameters can be simultaneously calibrated with simple on-site operations. Moreover, the calibration target used in this method is only a planar checkerboard, which can be easily acquired at low cost. It is verified in the experiment that the proposed method is efficient and accurate, with the calibration duration within 10 minutes and the measurement accuracy within 0.40mm. Additionally, object pose measurement experiment is conducted to validate the effectiveness of the proposed method in practical application.**

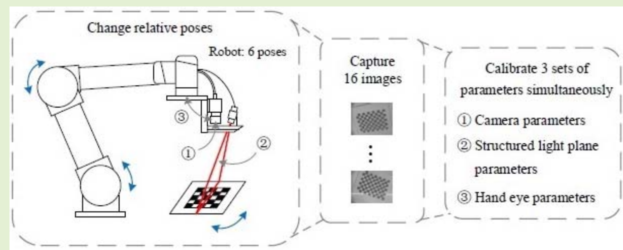

***Index Terms*— Robotic hand eye system, sensor calibration, simultaneous calibration, structured light vision.**

I. Introduction

NOWADAYS, 3-D perception system has become a crucial component in intelligent manufacturing. Since line structured light vision sensor possesses desirable characteristics of high precision and anti-interference capability, it has been selected as the automatic 3-D perception system in various industrial applications, including robotic bin-picking [1], on-machine inspection [2], robotic welding [3], [4], robotic grinding [5], etc. In these applications, the sensor is typically integrated with a robot to form a robotic hand eye system. However, the measurement range of the line structured light vision sensor is limited due to its field of view. In order to scan and measure the target in a larger work space, the line structured light vision sensor is generally installed on the end of a robotic manipulator and thus an eye-in-hand measurement system is established.

For the 3-D measurement using vision sensors, sensor calibration is an indispensable procedure [6]. Specifically, for line structured light vision sensor in robotic eye-in-hand system, there are three groups of parameters that need to be calibrated, which are camera parameters, hand eye parameters, and structured light plane (laser plane) parameters.

Camera parameters calibration has been extensively studied over the years [7]–[10]. These methods determine the intrinsic parameters as well as the extrinsic parameters of the camera using geometric constraints, and establish the mapping between 2-D image coordinate system and 3-D camera coordinate system or world coordinate system. Among them, the calibration method given by Zhang [9] using a planar checkerboard as calibration target is widely applied due to its flexibility and accuracy. This method only requires the

Manuscript received December 3, 2019; revised February 17, 2020; accepted February 18, 2020. Date of publication February 21, 2020; date of current version May 5, 2020. This work was supported in part by the National Natural Science Foundation of China under Grant U1813208 and Grant 61903362 and in part by the 2019 Youth Research Fund of the State Key Laboratory of Management and Control for Complex Systems under Grant 20190201. The associate editor coordinating the review of this article and approving it for publication was Dr. Rosario Morello. *(Corresponding author: Fengshui Jing.)*

Zhe Wang, Fengshui Jing, and Min Tan are with the State Key Laboratory of Management and Control for Complex Systems, Institute of Automation, Chinese Academy of Sciences, Beijing 100190, China, and also with the School of Artificial Intelligence, University of Chinese Academy of Sciences, Beijing 100049, China (e-mail: wangzhe2016@ia.ac.cn; fengshui.jing@ia.ac.cn; min.tan@ia.ac.cn).

Junfeng Fan and Sai Deng are with the State Key Laboratory of Management and Control for Complex Systems, Institute of Automation, Chinese Academy of Sciences, Beijing 100190, China (e-mail: fanjunfeng2014@ia.ac.cn; dengsai2012@ia.ac.cn).

Mingyang Zheng is with the School of Control and Computer Engineering, North China Electric Power University, Beijing 102206, China (e-mail: mingyang.zheng710@gmail.com).

Digital Object Identifier 10.1109/JSEN.2020.2975538

camera to capture the images of a planar target at different unknown poses. The analytical solution of the parameters can be obtained using the correspondence between the image and the target, and optimization method is adopted to refine the solution.

In order to determine the accurate relation between robot end coordinate and the camera coordinate, hand eye parameters calibration methods have been explored for decades [11]–[17]. Typically, these methods formulate the robotic hand eye calibration problem into solving $AX = XB$, where A and B represents the measured robot end movement and sensor movement, while X indicates the relative transformation between the robot and the sensor. By applying analytical or optimization methods, an estimation of unknown X can be derived. These methods provide a general way for both eye-in-hand and eye-to-hand calibration. In industrial applications, an alternative hand eye calibration method is contact calibration method [18]. In this method, the end effector of the robot needs to be precisely positioned at specific points on the calibration target that is previously measured by the sensor. By the registration of 3-D points given by the robot and the sensor, the hand eye relation can be determined. This method simplifies $AX = XB$ into a registration problem of 2 sets of 3-D points with known correspondence. However, this method only provides the transformation between the sensor and end effector instead of the robot end joint, and the end effector with a pointed end (*e.g.* a welding torch) is required for the contact calibration.

For structured light plane parameters calibration, there are a large number of researches conducted based on various kinds of calibration targets, including 3-D calibration block [19], ball target [20], multi-sphere board [21], planar line target [22] and concentric circle target [23]. In these methods, the equation of the structured light plane can be calculated based on the correspondence between the calibration target and structured light images. With the structured light plane equation, 3-D coordinate can be perceived by the sensor based on triangulation. However, in these methods, the specific calibration targets with high precision, especially 3-D targets, are difficult to acquire.

Traditionally, these three calibration procedures are conducted separately [24], [25], making the calibration process of the whole system time-consuming. To address this, some simultaneous calibration methods are proposed.

Fan *et al.* [26] proposed a simple calibration technique based on the calibration method of Zhang [9] using a planar checkerboard as calibration target. This technique achieves simultaneous calibration of camera parameters and structured light plane parameters without specially designed calibration target. However, the hand eye calibration still needs to be implemented individually in this method. Santolaria *et al.* [27] proposed a one-step method for the simultaneous intrinsic and extrinsic calibration of laser line scanner mounted on 3-DOF coordinate measuring machines (CMM). However, this method adopts a complex gauge object which is costly and inefficient to produce for the calibration. In addition, this method also utilizes the above mentioned contact calibration method for hand eye calibration. To accomplish this process, the sensor is

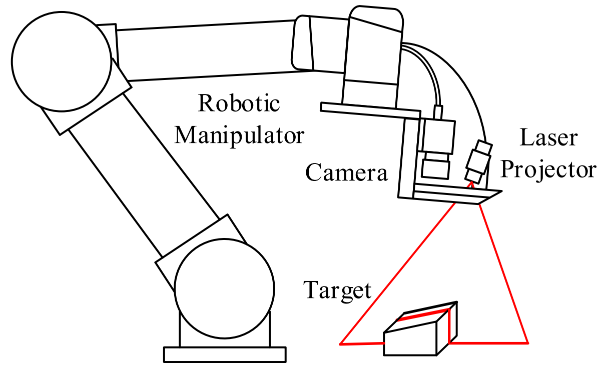

Fig. 1. The line structured light vision sensor in robotic eye-in-hand system.

replaced by a pointed end effector. Therefore, the calibration precision could be influenced by the machining error of the end effector as well as the installation error of the sensor after the calibration. Xie *et al.* [28] proposed a simultaneous intrinsic and extrinsic calibration method for structured light sensors on 3-DOF CMM. Because CMM only moves in three orthogonal directions with no rotation, the pose of the sensor is fixed in the base coordinate of CMM. Thus, the robot end coordinate is not established and the calibration method cannot be applied to the sensor mounted on 6-DOF robot with pose transformation.

Therefore, an efficient calibration method that is able to simultaneously conduct the three calibration procedures for structured light based eye-in-hand measurement system is yet to be fully accomplished.

In this study, we propose a highly efficient calibration method of line structured light vision sensor in robotic eye-in-hand system. This method is capable of calibrating the camera parameters, hand eye parameters, and structured light plane (laser plane) parameters simultaneously with simplified procedures. The calibration target of this method is a commonly used planar checkerboard, which can be readily acquired at low cost.

The remainder of this paper is organized as follows: Section II provides the description of the line structured light vision sensor in the robotic eye-in-hand system. Section III introduces the calibration framework and methods, including the definition of coordinate system, the parameters computation and the calibration pipeline. The experiments and results are presented in Section IV. The conclusion of this paper is drawn in Section V.

II. System Description

Generally, the line structured light vision sensor in a robotic eye-in-hand system is setup as illustrated in Fig. 1. The line structured light vision sensor consists of a line laser projector and a monocular industrial camera, both fixed on a supporting structure. The vision sensor is mounted on the end of a robotic manipulator. Carried by the robotic manipulator, the structured light vision sensor is capable of conducting measurement in a larger range.

In our structured light vision system, an optical filter and an optical dimmer are installed in front of the camera lens to filter out the light noises in the on-site measurement. The filter

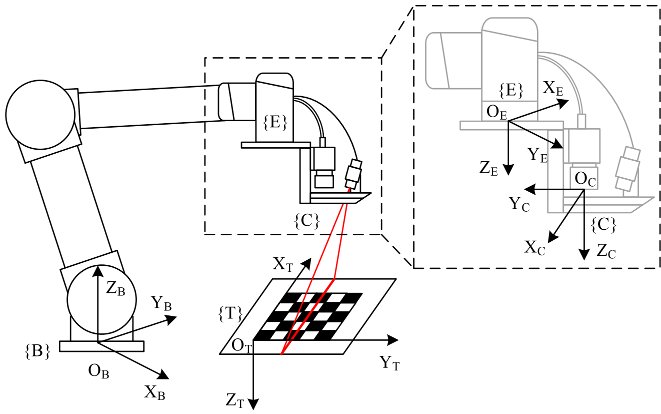

Fig. 2. The coordinate system definition.

and the dimmer are both devised as drawer-type. During the calibration process, the filter and the dimmer can be easily withdrew from the vision sensor to obtain a clear view of the calibration target.

The calibration target adopted in our experiment is a common planar checkerboard. Actually, for the proposed calibration method, other planar calibration targets (*e.g.* dotted planar target) used in camera calibration can also be adopted. During the calibration process, the calibration target is placed within the field of view of the camera on a platform and the laser stripe pattern is projected onto the calibration target.

III. Calibration Framework and Methods

A. Coordinate System

In this paper, the coordinate system consists of robot base coordinate system {B}, robot end coordinate system {E}, camera coordinate system {C}, and target coordinate system {T}, as shown in Fig. 2.

${}^1_2M$ in special Euclidean group $SE(3)$ is defined as the homogeneous transformation matrix of coordinate system 2 in coordinate system 1, with the form of

$$ {}^1_2M = \begin{pmatrix} {}^1_2R & {}^1t_2 \\ 0 & 1 \end{pmatrix}, \tag{1} $$

where ${}^1_2R$ is a rotation matrix in special orthogonal group $SO(3)$, and ${}^1t_2$ is a translation vector in R^3.

The main purpose of the line structured light vision sensor in robotic eye-in-hand system is to conduct the 3-D measurement of the target in a fixed coordinate system. For the convenience of robotic manipulation guided by the measured information, the measurement result in the robot base coordinate system is required to be provided by the measurement system. Therefore, the measurement result ${}^B_TM$ from {B} to {T} is calculated as follows:

$$ {}^B_TM = {}^B_EM\, {}^E_CM\, {}^C_TM, \tag{2} $$

where ${}^B_EM$ is the transformation from robot base to robot end coordinate system which can be acquired from the forward kinematics of the robotic manipulator and is normally provided by the robot interface. ${}^E_CM$ is the transformation from robot end to camera coordinate system, which needs to be calibrated by hand eye calibration. ${}^C_TM$ is the transformation from camera to target coordinate system, which can be calculated by image processing along with the calibrated camera calibration parameters and structured light plane parameters.

In the calibration process, the target coordinate system {T} is set at the corner of the checkerboard calibration target, and moves together with the calibration target. In the proposed calibration method, the camera parameters are firstly calibrated. The structured light plane parameters and hand eye parameters are derived using the camera calibration results.

B. Camera Parameters

Intrinsic matrix of camera can be formulated as follows:

$$ \begin{pmatrix} u \\ v \\ 1 \end{pmatrix} = \frac{1}{z_c} \begin{pmatrix} k_x & s & u_0 \\ 0 & k_y & v_0 \\ 0 & 0 & 1 \end{pmatrix} \begin{pmatrix} x_c \\ y_c \\ 1 \end{pmatrix}, \tag{3} $$

where (u,v) denotes the 2-D point in image coordinate with the principle point of (u_0,v_0), s is the skew of two axes of image coordinate, k_x and k_y are the scale factors of the two axes, and (x_c,y_c,z_c) is the 3-D point in camera coordinate system.

Extrinsic matrix of camera can be formulated as follows:

$$ \begin{pmatrix} x_c \\ y_c \\ z_c \\ 1 \end{pmatrix} = {}^T_CM \begin{pmatrix} x_t \\ y_t \\ z_t \\ 1 \end{pmatrix}, \tag{4} $$

where

$$ {}^T_CM = \begin{pmatrix} {}^T_CR & {}^Tt_C \\ 0 & 1 \end{pmatrix} = \begin{pmatrix} n_x & o_x & a_x & p_x \\ n_y & o_y & a_y & p_y \\ n_z & o_z & a_z & p_z \\ 0 & 0 & 0 & 1 \end{pmatrix}. \tag{5} $$

By applying method in [9], or other camera calibration methods as well, the intrinsic matrix of the camera and the extrinsic matrices ${}^T_CM$ of camera corresponding to different poses of calibration target can be determined. With the intrinsic parameters in (3), point (x_c,y_c,z_c) in camera coordinate system can be calculated using coordinate (u,v) in image coordinate system.

$$ y_c = \frac{z_c}{k_y}(v - v_0). \tag{6} $$

$$ x_c = \frac{z_c}{k_x}(u - u_0 - \frac{s}{k_y}(v - v_0)). \tag{7} $$

The value of z_c can be obtained using point (x_t, y_t, z_t) and extrinsic parameters. According to the coordinate definition of the calibration target Fig. 2, noticing the target is a planar checkerboard, the value of z_t of a point on the calibration target is 0. Thus we obtain

$$ \begin{pmatrix} {}^T_CR & {}^Tt_C \\ 0 & 1 \end{pmatrix}^{-1} \begin{pmatrix} x_c \\ y_c \\ z_c \\ 1 \end{pmatrix} = \begin{pmatrix} x_t \\ y_t \\ 0 \\ 1 \end{pmatrix}, \tag{8} $$

which can be rewrite as follows:

$$\begin{pmatrix} n_x & n_y & n_z & -p_xn_x - p_yn_y - p_zn_z \\ o_x & o_y & o_z & -p_xo_x - p_yo_y - p_zo_z \\ a_x & a_y & a_z & -p_xa_x - p_ya_y - p_za_z \\ 0 & 0 & 0 & 1 \end{pmatrix} \begin{pmatrix} x_c \\ y_c \\ z_c \\ 1 \end{pmatrix} = \begin{pmatrix} x_t \\ y_t \\ 0 \\ 1 \end{pmatrix}. \quad (9)$$

Thus, combining (6), (7) and (9), for all the points on the calibration target, we obtain

$$z_c = \frac{p_xa_x + p_ya_y + p_za_z}{\frac{a_x}{k_x}(u-u_0) + \frac{1}{k_y}(a_y - \frac{a_x}{k_x}s)(v-v_0) + a_z}. \quad (10)$$

C. Structured Light Plane Calibration

In camera coordinate system, all the points on the line laser stripe pattern are on the structured light plane, which is a spatial plane formulated as follows:

$$z_c = l_1x_c + l_2y_c + l_3, \quad (11)$$

where l_1, l_2 and l_3 are the spatial plane parameters.

In the calibration process, the laser stripe is projected on the calibration target. Therefore, for all the points on the laser stripe pattern, the equation (6), (7) and (10) holds. In image coordinate system, the position values of points (u,v) on the laser stripe can be extracted using image processing methods such as gradient calculation [29] or gray centroid method [3].

With sufficient amount of laser stripe points (x_c, y_c, z_c) computed using the equation (6), (7) and (10) along with corresponding (u,v) values, the value of l_1, l_2 and l_3 in (11) can be obtained by solving the linear equation:

$$Ax = b, \quad (12)$$

where

$$A = \begin{pmatrix} x_{c_1} & y_{c_1} & 1 \\ \vdots & \vdots & \vdots \\ x_{c_i} & y_{c_i} & 1 \\ \vdots & \vdots & \vdots \\ x_{c_n} & y_{c_n} & 1 \end{pmatrix}, \; x = \begin{pmatrix} l_1 \\ l_2 \\ l_3 \end{pmatrix}, \; b = \begin{pmatrix} z_{c_1} \\ \vdots \\ z_{c_i} \\ \vdots \\ z_{c_n} \end{pmatrix}. \quad (13)$$

If $n > 3$ and $rank(A, b) = 3$, a least square solution can be given as:

$$x = (A^TA)^{-1}A^Tb. \quad (14)$$

Thus the structured light plane parameters in camera coordinate can be determined by more than 3 non-collinear laser stripe points. Accordingly, the laser stripe points adopted to calculate the plane parameters need to be collected from laser stripe images with different calibration target pose.

During the on-site measurement of structured light sensor, the extrinsic parameters are unknown. Therefore, the laser stripe point (x_c, y_c, z_c) in camera coordinate system needs to be solved using equation (6), (7) and (11). The formulation of z_c becomes:

$$z_c = \frac{l_3k_xk_y}{k_xk_y + l_1k_y(u_0 - u) + (l_2k_x - l_1s)(v_0 - v)}. \quad (15)$$

Thus, the 3-D coordinates of the laser stripe pattern points on the target in camera coordinate can be computed using the known camera intrinsic parameters and structured light plane parameters.

D. Eye in Hand Calibration

During hand eye calibration, the orientation and position of the calibration target is fixed on the operation platform. Thus the target coordinate system is unchanged in the robot base coordinate system. If the pose and position of the target is measured by two different camera views i and j controlled by the robotic manipulator, we obtain:

$${}^B_TM = {}^B_EM_i {}^E_CM {}^C_TM_i = {}^B_EM_j {}^E_CM {}^C_TM_j. \quad (16)$$

For k pairs of camera views, the following equation holds:

$$({}^B_EM_j^{-1} {}^B_EM_i)_k {}^E_CM = {}^E_CM ({}^C_TM_j {}^C_TM_i^{-1})_k. \quad (17)$$

Since ${}^B_EM$ can be acquired from the robotic manipulator interface and the ${}^C_TM$ is the inverse of the extrinsic matrix of camera to each calibration target, the hand eye matrix ${}^E_CM$ can be obtained by solving $AX = XB$, where A and B are both known in the aforementioned calibration process.

By applying method proposed by Tsai and Lenz [13], or other methods of solving hand eye relation equation as well, hand eye matrix ${}^E_CM$ can be calculated. It is worth noticing that at least 3 different camera views need to be required to form 2 corresponding pairs of camera views for a stable solution.

E. Calibration Process

The whole calibration process can be divided into on-site operation and calculation process.

In the first step of on-site operation, the robotic manipulator is firstly fixed at a referenced pose (pose I). As illustrated in the pose I of Fig. 3, the camera is right above the calibration target on the operation platform. With the camera fixed in this pose, the pose of the calibration target is manually changed several times within the field of view of the camera, and a target picture is captured for each target pose. These pictures are used to calibrate the camera parameters, so the laser projector is turned off during this process. For the robustness of calibration, at least 4 pictures of different target poses need to be captured for calibration.

In the second step of on-site operation, the calibration target is fixed on the platform at certain pose. Then, the manipulator, along with the camera, is moved to 6 distinct poses, keeping the calibration target in the field of view. In order to reduce the error, the poses are set as shown in Fig. 3, as suggested by [13]. In each pose, two pictures are captured. The first picture is a clear view of the target and the second view is the image of the target with structured light (laser stripe pattern)

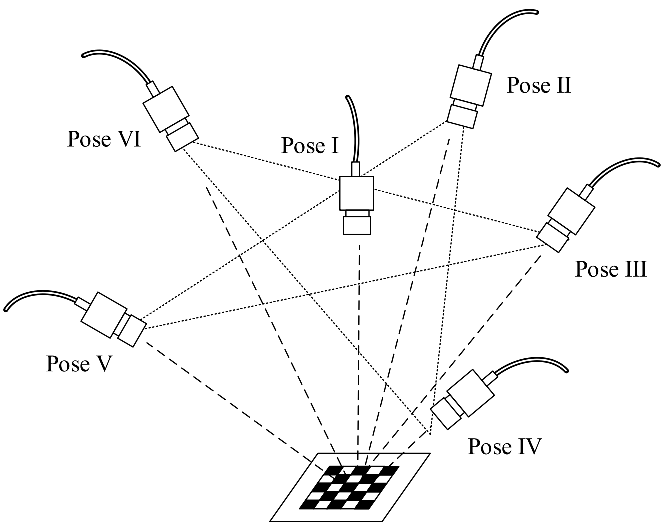

Fig. 3. The camera poses in on-site calibration.

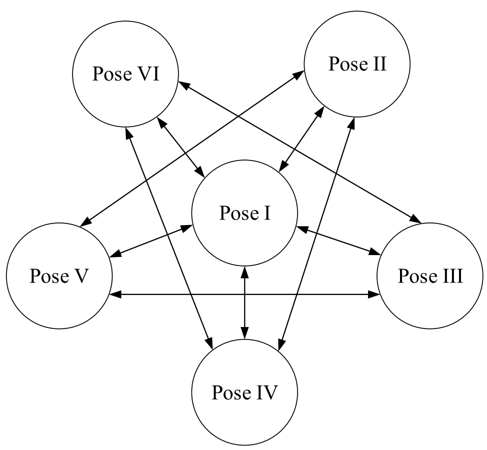

Fig. 4. The formulation of 10 pose pairs.

projected on it. So the laser projector is switched on and off during the process. The clear view pictures of the target are used in camera calibration combining with the pictures captured in the first step. With the calibrated extrinsic parameters, these pictures also provide ${}^{C}_{T}M$ in the hand eye calibration. The structured light pictures, along with corresponding ${}^{C}_{T}M$, are used for structured light plane calculation.

During the calculation process, the calibration target pictures from the previous two steps with no structured light on it are used to calibrate the intrinsic parameters of the camera as well as the extrinsic parameters to each relative pose. Next, combining the 6 pictures with structured light pattern captured in the second step and the corresponding 6 relative poses from the calibrated extrinsic parameters, the structured light plane can be fitted. Finally, the 6 camera poses ${}^{C}_{T}M$ from extrinsic parameters, combined with 6 robot end pose ${}^{B}_{E}M$ given by the manipulator, can be formulated to 10 pairs of pose relations in the calculation of $AX = XB$, with the pose disparity relatively large within each pair, as shown in Fig. 4.

The flowchart of the calibration process is illustrated in Fig. 5. In this calibration process, the on-site operation is relatively simple and efficient. In total, merely 6 robot poses and 16 pictures are enough for the calibration of all the three sets of parameters using only a planar checkerboard as target.

IV. Experiments

A. Experiment Configuration

The experiment configuration is presented in Fig. 6.

In the experiment, a UR5 cooperative robot is used as the robotic manipulator. The industrial camera on the line structured light vision sensor is MER-134-93U3M CMOS camera from DAHENG IMAGING, the resolution of which is 1280 × 1024. The lens on the camera is M1214-MP2 from Computar. The laser projector is 635nm wavelength line projector from Anford. The calibration target is a planar checkerboard with 9 rows and 12 columns of grids with the side length of 10mm.

B. Calibration Results

To verify the effectiveness of the proposed method, a calibration experiment has been conducted. In this experiment, the manipulator was moved to 6 different poses and a total of 16 pictures were taken, as mentioned in the calibration process. The whole on-site calibration and data collection procedures were finished within 10 minutes by one person, and the duration could be further reduced if the operator is proficient.

During the calculation, firstly, the camera intrinsic and extrinsic parameters were calculated with 10 pictures of target without structured light pattern. The intrinsic parameters were:

$$\begin{pmatrix} 2545.694 & 0.005 & 637.162 \\ 0 & 2545.396 & 509.826 \\ 0 & 0 & 1 \end{pmatrix}, \tag{18}$$

where the parameters corresponded to those in the intrinsic matrix of (3).

Then, using the calibrated camera parameters and the 6 structured light pattern images, the structured light plane was obtained as follows:

$$z_c = 0.020x_c + 5.269y_c + 167.335. \tag{19}$$

Finally, using the 6 poses of robot end ${}^{B}_{E}M$ and the corresponding 6 sets of camera extrinsic parameters ${}^{C}_{T}M$, the hand eye matrix ${}^{E}_{C}M$ was given as:

$${}^{E}_{C}M = \begin{pmatrix} -0.7009 & -0.7132 & 0.0132 & 141.8965 \\ 0.7130 & -0.7010 & -0.0149 & 75.8074 \\ 0.0199 & -0.0011 & 0.9998 & 51.6516 \\ 0 & 0 & 0 & 1 \end{pmatrix}, \tag{20}$$

where the translation ${}^{E}t_{C}$ was measured in millimeters.

C. Calibration Accuracy Verification

In order to verify the accuracy of the proposed method, an accuracy verification experiment was conducted. In this experiment, a checkerboard target was fixed on the platform and the relation between the target and robot base was fixed.

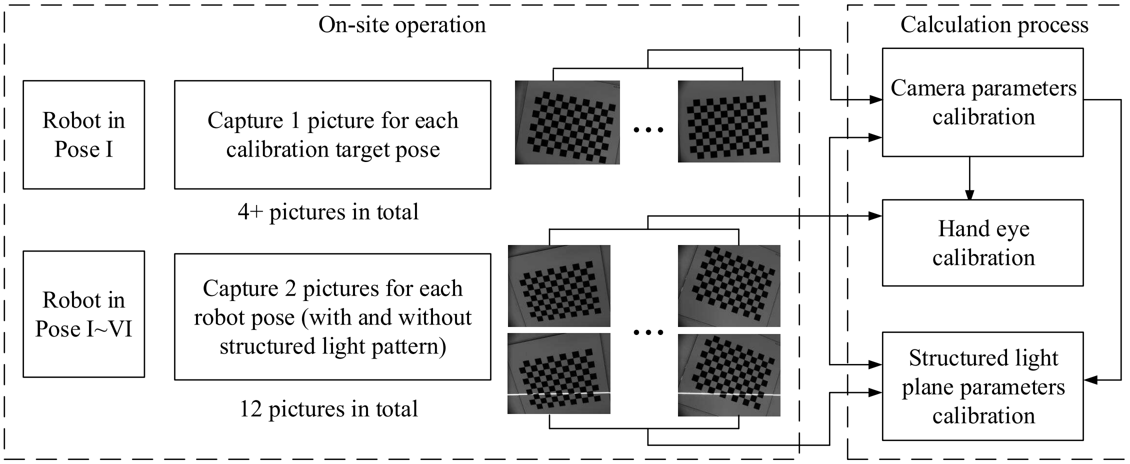

Fig. 5. The flow chart of the calibration process.

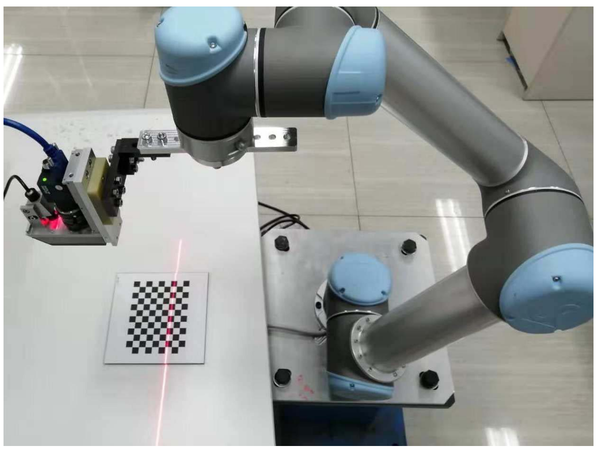

Fig. 6. The experiment configuration.

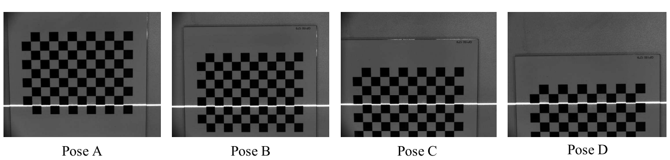

Fig. 7. The experiment pictures (with calibration target pose fixed).

TABLE I
THE ROBOT END POSE IN THE VERIFICATION EXPERIMENT

Pose	T_x(mm)	T_y(mm)	T_z(mm)	R_x(rad)	R_y(rad)	R_z(rad)
Pose A	55.79	201.58	649.27	2.2410	2.2133	-0.1324
Pose B	56.34	203.21	657.34	2.2489	2.2201	-0.0479
Pose C	88.94	230.25	647.45	2.2313	2.2086	-0.1480
Pose D	90.10	234.74	651.33	2.2633	2.2215	-0.0790

Adjusting the pose of the manipulator, the line laser stripe pattern was projected onto the side of the grids on the checkerboard. The pose was adjusted 4 times and interval between each structured light pattern is 20mm, as shown in Fig. 7. And the corresponding robot end pose is demonstrated in Table I, where the rotation is presented using equivalent angle-axis representation.

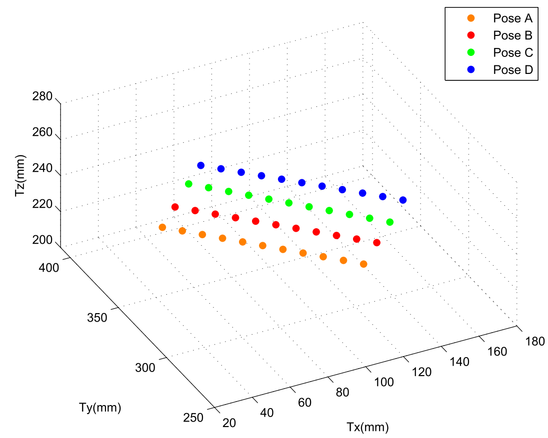

Fig. 8. The measured 3-D points.

TABLE II
THE MEASUREMENT ERROR IN THE VERIFICATION EXPERIMENT

	Average Error	Standard Deviation
Interval Measurement Error	0.125mm	0.093mm
Plane Fitting Error	0.210mm	0.190mm

The intersection points of grid corners and line structured light patterns were extracted to compute the measured interval distance in robot base coordinate system, using the calibration parameters. In total, 44 intersection points were measured. The measured 3-D intersection points corresponding to 4 poses are illustrated in Fig. 8. The average measurement error of the interval between neighboring poses and its standard deviation value is presented in Table II. The errors of each measured interval distance are presented in Fig. 9.

Furthermore, the plane equation of the measured 3-D intersection points in robot base coordinate is fitted using least square fitting.

$$z_b = -0.016x_b + 0.000y_b + 244.851 \tag{21}$$

Then, the errors measured by Euclidean distances from the measured 3-D points to the plane are calculated. The average

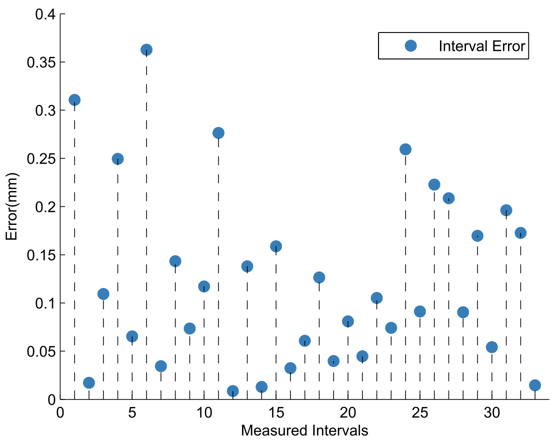

Fig. 9. The measured interval distance.

Fig. 10. Pose measurement experiment setup.

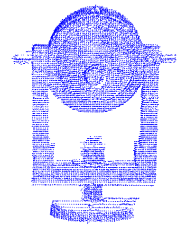

Fig. 11. The 3-D point cloud of target.

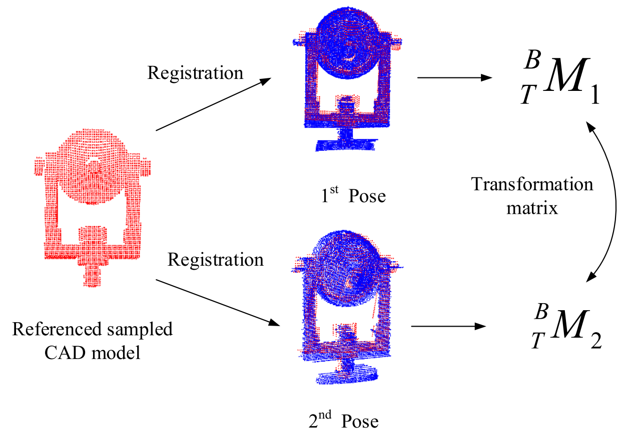

Fig. 12. The pose measurement experiment pipeline.

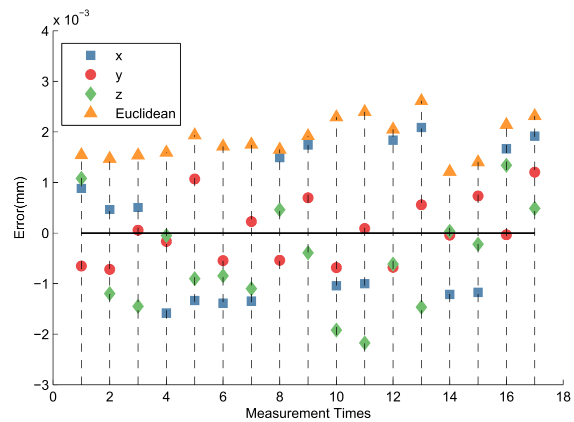

Fig. 13. The translation error distribution in pose measurement.

error is 0.210mm with standard deviation value of 0.190mm, as presented in Table II.

As verified in this experiment, the measurement error of proposed calibration method was within 0.40mm, demonstrating desirable accuracy. It is worth noticing that the positional repeatability of the manipulator in this experiment is 0.1mm, so the result might be further promoted when the sensor is integrated with an industrial robot with higher precision.

D. Pose Measurement Experiment

In order to evaluate the practical performance of the eye-in-hand measurement system after calibration, an object pose measurement experiment has been conducted. As shown in Fig. 10, a prism target for total station was adopted as the target to be measured.

In the pose measurement experiment, the target was placed on a rotary platform and was scanned by the line structured light sensor on the manipulator. With the calibration parameters and robot end poses, the 3-D coordinates of the laser stripe on every frame of the structured light image were obtained, and the 3-D points were combined into a point cloud. After the removal of abnormal points caused by reflection using point cloud filters, the 3-D point cloud of the target in robot base coordinate was reconstructed as presented in Fig. 11.

Then, as demonstrated in Fig. 12, the 3-D point cloud was registered with the referenced CAD model of the target using ICP registration [30]. The referenced CAD model was set at the origin of the robot base coordinate system in a upright pose, and was cropped and sampled into referenced point cloud. After the registration, the resulting transformation was the measured pose of the target in robot base coordinate. After the first measurement, the target was horizontally rotated 10° by its center, and was scanned again. The second point cloud was then registered again with the CAD model to obtain the second pose measurement. Then the transformation between two measured poses was computed. This pose measurement pipeline was repeated several times to validate the pose measurement accuracy. The transformation errors including translation and rotation errors are illustrated in Fig. 13

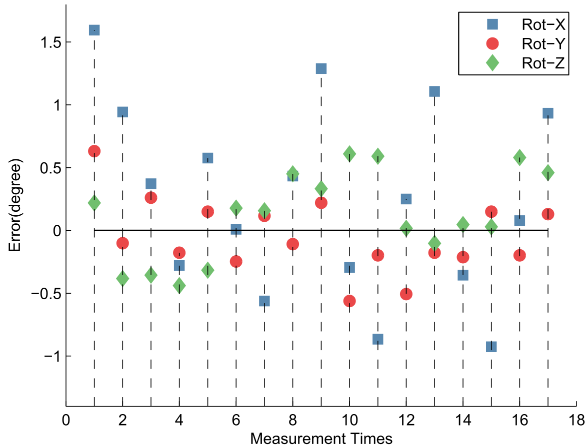

Fig. 14. The rotation error distribution in pose measurement.

TABLE III
THE POSE MEASUREMENT RESULT: TRANSLATION ERROR

	Trans-X	Trans-Y	Trans-Z	Trans-E
Average Error	1.334mm	0.511mm	0.925mm	1.855mm

TABLE IV
THE POSE MEASUREMENT RESULT: ROTATION ERROR

	Rot-X	Rot-Y	Rot-Z
Average Error	0.639°	0.244°	0.310°

and Fig. 14. The average transformation errors are listed in Table III and Table IV. In Table III, Trans-X, Trans-Y, Trans-Z, and Trans-E stand for translation error in X, Y, Z axis and Euclidean metric. In Table IV, rotations are interpreted into Z-Y-X Euler angle representation, while Rot-X, Rot-Y, and Rot-Z stand for rotation error of X, Y, and Z axis. It is shown that the pose measurement is accurate, even partially affected by the registration error brought by the registration method. Therefore, the proposed efficient calibration method can be practically utilized in the 3-D measurement system.

V. CONCLUSION

In this paper, we present an efficient calibration method of line structured light vision sensor in robotic eye-in-hand system. This method can be adopted to simultaneously calibrate camera parameters, robot hand eye parameters and structured light plane parameters with minimal on-site operations using a simple planar calibration target. The calibration process can be accomplished within 10 minutes, which is highly efficient for the calibration of structured light hand eye system. An accuracy verification experiment and a practical object pose measurement experiment are conducted, suggesting that the proposed method is accurate and effective.

From the aforementioned experiment results and analyses, the proposed method possesses two properties that contribute to its efficiency, accuracy and effectiveness.

Firstly, in this method, the extrinsic parameters calculated in the camera calibration are used in the calibration of hand eye parameters as well as the structured light plane parameters. This largely reduces the on-site operations during the data collection process for calibration. Moreover, the extrinsic parameters enable the structured light plane to be calibrated without special designed calibration target, making the procedure efficient.

Secondly, since the on-site operation is made simultaneously for three sets of parameters, the deviations caused by different environment conditions during separate calibration are avoided. Using simultaneous method, the possibility that one set of parameters might change during the calibration of another in the separate calibration is eliminated. Therefore, the proposed method is more robust and accurate in the practical applications.

In the future, this method is expected to be adopted by line structured light hand eye measurement systems in actual industrial applications to improve the efficiency and productivity of the manufacturing process. For the complex tasks that demand higher accuracy, an industrial robot with higher precision, a line laser projector with thinner laser stripe pattern, and a camera with higher resolution can be adopted to further improve the accuracy of the system, while calibration procedures remain the same.

REFERENCES

[1] W.-C. Chang and C.-H. Wu, "Eye-in-hand vision-based robotic bin-picking with active laser projection," *Int. J. Adv. Manuf. Technol.*, vol. 85, nos. 9–12, pp. 2873–2885, 2016.
[2] N. D. M. Phan, Y. Quinsat, and C. Lartigue, "Optimal scanning strategy for on-machine inspection with laser-plane sensor," *Int. J. Adv. Manuf. Technol.*, vol. 103, nos. 9–12, pp. 4563–4576, May 2019.
[3] J. Fan, F. Jing, L. Yang, L. Teng, and M. Tan, "A precise initial weld point guiding method of micro-gap weld based on structured light vision sensor," *IEEE Sensors J.*, vol. 19, no. 1, pp. 322–331, Jan. 2019.
[4] J. Muhammad, H. Altun, and E. Abo-Serie, "Welding seam profiling techniques based on active vision sensing for intelligent robotic welding," *Int. J. Adv. Manuf. Technol.*, vol. 88, nos. 1–4, pp. 127–145, 2017.
[5] H. Xie, C.-T. Pang, W.-L. Li, Y.-H. Li, and Z.-P. Yin, "Hand-eye calibration and its accuracy analysis in robotic grinding," in *Proc. IEEE Int. Conf. Automat. Sci. Eng. (CASE)*, Aug. 2015, pp. 862–867.
[6] S. Kong, X. Fang, X. Chen, Z. Wu, and J. Yu, "A NSGA-II-based calibration algorithm for underwater binocular vision measurement system," *IEEE Trans. Instrum. Meas.*, vol. 69, no. 3, pp. 794–803, Mar. 2020.
[7] Y. I. Abdel-Aziz and H. M. Karara, "Direct linear transformation from comparator coordinates into object space coordinates in close-range photogrammetry," *Photogramm. Eng. Remote Sens.*, vol. 81, no. 2, pp. 103–107, Feb. 2015.
[8] R. Tsai, "A versatile camera calibration technique for high-accuracy 3D machine vision metrology using off-the-shelf TV cameras and lenses," *IEEE J. Robot. Autom.*, vol. RA-3, no. 4, pp. 323–344, Aug. 1987.
[9] Z. Zhang, "A flexible new technique for camera calibration," *IEEE Trans. Pattern Anal. Mach. Intell.*, vol. 22, no. 11, pp. 1330–1334, Nov. 2000.
[10] X. Meng and Z. Hu, "A new easy camera calibration technique based on circular points," *Pattern Recognit.*, vol. 36, no. 5, pp. 1155–1164, May 2003.
[11] M. Shah, R. D. Eastman, and T. Hong, "An overview of robot-sensor calibration methods for evaluation of perception systems," in *Proc. Workshop Perform. Metrics Intell. Syst. (PerMIS)*, 2012, pp. 15–20.
[12] Y. C. Shiu and S. Ahmad, "Calibration of wrist-mounted robotic sensors by solving homogeneous transform equations of the form AX=XB," *IEEE Trans. Robot. Autom.*, vol. 5, no. 1, pp. 16–29, Feb. 1989.
[13] R. Y. Tsai and R. K. Lenz, "A new technique for fully autonomous and efficient 3D robotics hand/eye calibration," *IEEE Trans. Robot. Autom.*, vol. 5, no. 3, pp. 345–358, Jun. 1989.

[14] F. C. Park and B. J. Martin, "Robot sensor calibration: Solving AX=XB on the Euclidean group," *IEEE Trans. Robot. Autom.*, vol. 10, no. 5, pp. 717–721, Oct. 1994.
[15] N. Andreff, R. Horaud, and B. Espiau, "On-line hand-eye calibration," in *Proc. IEEE Int. Conf. 3-D Digit. Imag. Modeling*, Oct. 1999, pp. 430–436.
[16] Z. Zhao, "Hand-eye calibration using convex optimization," in *Proc. IEEE Int. Conf. Robot. Automat.*, May 2011, pp. 2947–2952.
[17] J. Wu, Y. Sun, M. Wang, and M. Liu, "Hand-eye calibration: 4D procrustes analysis approach," *IEEE Trans. Instrum. Meas.*, to be published.
[18] G. A. Idrobo-Pizo, J. M. S. T. Motta, and R. C. Sampaio, "A calibration method for a laser triangulation scanner mounted on a robot arm for surface mapping," *Sensors*, vol. 19, no. 8, p. 1783, Apr. 2019.
[19] D. Q. Huynh, "Calibration of a structured light system: A projective approach," in *Proc. IEEE Conf. Comput. Vis. Pattern Recognit.*, Jun. 1997, pp. 225–230.
[20] Z. Liu, X. Li, F. Li, and G. Zhang, "Calibration method for line-structured light vision sensor based on a single ball target," *Opt. Lasers Eng.*, vol. 69, pp. 20–28, Jun. 2015.
[21] J. Xu, J. Douet, J. Zhao, L. Song, and K. Chen, "A simple calibration method for structured light-based 3D profile measurement," *Opt. Laser Technol.*, vol. 48, pp. 187–193, Jun. 2013.
[22] Z. Wei, C. Li, and B. Ding, "Line structured light vision sensor calibration using parallel straight lines features," *Optik*, vol. 125, no. 17, pp. 4990–4997, Sep. 2014.
[23] M. Shao, J. Dong, and A. H. Madessa, "A new calibration method for line-structured light vision sensors based on concentric circle feature," *J. Eur. Opt. Soc.-Rapid Publications*, vol. 15, no. 1, p. 1, Jan. 2019.
[24] Y. Qi, F. Jing, and M. Tan, "Line-feature-based calibration method of structured light plane parameters for robot hand-eye system," *Opt. Eng.*, vol. 52, no. 3, Mar. 2013, Art. no. 037202.
[25] N. Mu, K. Wang, Z. Xie, and P. Ren, "Calibration of a flexible measurement system based on industrial articulated robot and structured light sensor," *Opt. Eng.*, vol. 56, no. 5, May 2017, Art. no. 054103.
[26] J. Fan, F. Jing, Z. Fang, and Z. Liang, "A simple calibration method of structured light plane parameters for welding robots," in *Proc. 35th Chin. Control Conf. (CCC)*, Jul. 2016, pp. 6127–6132.
[27] J. Santolaria, J. J. Pastor, F. J. Brosed, and J. J. Aguilar, "A one-step intrinsic and extrinsic calibration method for laser line scanner operation in coordinate measuring machines," *Meas. Sci. Technol.*, vol. 20, no. 4, Mar. 2009, Art. no. 045107.
[28] Z. Xie, X. Wang, and S. Chi, "Simultaneous calibration of the intrinsic and extrinsic parameters of structured-light sensors," *Opt. Lasers Eng.*, vol. 58, pp. 9–18, Jul. 2014.
[29] Z. Wang, F. Jing, and J. Fan, "Weld seam type recognition system based on structured light vision and ensemble learning," in *Proc. IEEE Int. Conf. Mechatronics Automat. (ICMA)*, Aug. 2018, pp. 866–871.
[30] P. J. Besl and N. D. McKay, "A method for registration of 3-D shapes," *IEEE Trans. Pattern Anal. Mach. Intell.*, vol. 14, no. 2, pp. 239–256, Feb. 1992.

Zhe Wang received the B.S. degree in automation from Nankai University, Tianjin, China, in 2016. He is currently pursuing the Ph.D. degree in control theory and control engineering with the State Key Laboratory of Management and Control for Complex Systems, Institute of Automation, Chinese Academy of Sciences, and the School of Artificial Intelligence, University of Chinese Academy of Sciences, Beijing, China. His current research interests include machine vision and robotics.

Junfeng Fan received the B.S. degree in mechanical engineering and automation from the Beijing Institute of Technology, Beijing, China, in 2014, and the Ph.D. degree in control theory and control engineering from the Institute of Automation, Chinese Academy of Sciences (IACAS), Beijing, in 2019. He is currently an Assistant Professor with IACAS. His research interests include industrial robotics, robot vision, and welding automation.

Fengshui Jing received the B.S. degree in mining engineering from Huainan Mining Institute, Anhui, China, in 1991, the M.S. degree in safety technology and engineering from Shandong Mining Institute, Shandong, in 1994, and the Ph.D. degree in control theory and control engineering from the Institute of Automation, Chinese Academy of Sciences (IACAS), Beijing, China, in 2002. From 1994 to 1999, he was an Assistant Professor with the Mechanical and Electrical Engineering Department, Shandong Agricultural University, Shandong. He is currently a Professor with the State Key Laboratory of Management and Control for Complex Systems, IACAS, and the School of Artificial Intelligence, University of Chinese Academy of Sciences, Beijing. His research interests include robotics, computer vision, and manufacturing systems.

Sai Deng received the B.S. degree in automation from Xiangtan University, Hunan, China, in 2012, and the Ph.D. degree in control theory and control engineering from the Institute of Automation, Chinese Academy of Sciences (IACAS), Beijing, China, in 2018. He is currently an Associate Professor with IACAS. His research interest includes motion control of the robot.

Mingyang Zheng is currently pursuing the B.S. degree in measurement and control technology and instrumentation with the School of Control and Computer Engineering, North China Electric Power University, Beijing, China. His current research interests include vision sensing and robotics.

Min Tan received the B.S. degree in control engineering from Tsinghua University, Beijing, China, in 1986, and the Ph.D. degree in control theory and control engineering from the Institute of Automation, Chinese Academy of Sciences, Beijing, in 1990. He is a Professor with the State Key Laboratory of Management and Control for Complex Systems, Institute of Automation, Chinese Academy of Sciences, and the School of Artificial Intelligence, University of Chinese Academy of Sciences, Beijing. His research interests include advanced robot control, multirobot systems, biomimetic robots, and manufacturing systems.